polymer papers

Small defects in crystalline polyethylene

Darrell H. Reneker and Jacob Mazur
Polymers Division, National Bureau of Standards, Gaithersburg, Maryland 20899 USA
(Received 20 May 1987; accepted 5 June 1987)

A family of five crystallographic defects of three classes (two dislocations, two dispirations and one disclination) which primarily involve only one polymer chain is described for polyethylene. The extra energy associated with each defect in a perfect polyethylene crystal was computed. The crystal model used consisted of a central chain containing the defect with 18 zig-zag chains in two shells around the central chain. The zig-zag chains each had 60 carbon atoms. The conformation of each defect, placed near the centre of the central chain, was adjusted to minimize the sum of the interatomic interactions. A closely related procedure was used to calculate the energy per chain at boundaries where each chain contains an identical 'partial' dislocation or disclination. The characterization of these well defined defects and partial defects greatly simplifies the establishment of connections between atomic and macroscopic scale phenomena in crystalline polyethylene.

(Keywords: crystal defect; dispiration; disclination; dislocation; polymer crystal; polymer conformations; polyethylene; chain twist boundary; free volume; transport processes; interstitial; vacancy; defect loops; defect lines; partial defect)

INTRODUCTION

This paper summarizes the properties of crystallographic defects in polyethylene. An important consequence of the identification and characterization of these defects is that the behaviour of larger volumes of material can then be related to atomistic parameters through the Brownian motion, the response to strain fields and other properties of entire defects. This greatly simplifies the development of models for the macroscopic behaviour of solid polyethylene and other polymers. It also provides guidance for the construction of detailed but manageable models for the incorporation of side branches into the crystal and for the interactions of various kinds of defects with morphological features such as folds.

The use of the word defect to name these nanometre scale structures arises from the viewpoint of the perfect crystal lattice. While this language is retained, the possibility of forming these structures is an inherent feature of the crystal. Each defect has a specific low energy conformation, and can be expected to occur whenever a sufficient amount of energy is available in a polyethylene crystal. The defects allow things to happen inside polyethylene crystals that would not happen if defects did not exist. The defects become the nanometre scale molecular mechanisms that diffuse along the molecules and translate them, rotate them, transfer free volume, accommodate structural singularities, bring reactive sites together, and more. In concert with a hierachy of larger structures, they mediate the physical properties of polyethylene. They are not restricted to polyethylene, and can be generalized to all other crystalline polymers. They even provide models of mechanisms which are likely to be important in the function of polymeric structures encountered in biology.

Earlier work on the defects is described in references cited below. The partial dislocation boundary is described here for the first time. Conformational calculations have been done for some of these defects in a variety of smaller models. The results that follow provide an accurate comparison of the energy and other properties of the defects in the same relatively large crystal model.

The five crystallographic defects considered here are:

(1) Dispiration loops (a) interstitial-like[1], (b) vacancy-like[2,3].
(2) Disclination loop[4].
(3) Dislocation loop (a) interstitial-like[4], (b) vacancy-like[5].

The word 'loop' connects the names to the terminology that has been established for larger defects in crystals of low molecular weight substances. That connection is described in detail by Reneker and Mazur[6]. In the remainder of this paper the word 'loop' is usually omitted for brevity. The atoms surrounding a crystallographic defect are found closer to lattice sites as the distance from the centre of the defect increases. This is not the case for partial defects, which cannot exist independently inside crystals, but are useful since they can combine to form crystallographic defects or special kinds of boundaries.

The partial defects discussed here are:

(4) Chain twist boundary (180°)[4].
(5) Chain twist boundary (90°)[4].
(6) Partial dislocation boundary.

The partial dislocation boundary for which computations were made contains an extra carbon atom in the boundary and is therefore interstitial-like. The vacancy-like partial dislocation boundary was not modelled. It is a long defect, with a high energy, and it is unstable when the end constraints are removed. Its conformation is a stretched zig-zag similar to the vacancy-like dislocation.

Larger defects, such as a loop that encircles two or more chains are also not included here. An example is the array of jog-like conformations which was identified by Predecki and Statton[7] as a screw dislocation associated with chain ends. There appear to be many other interesting, important and tractable but as yet undescribed interactions of crystallographic defects.

0032-3861/88/010003-11$03.00
© 1988 Butterworth & Co. (Publishers) Ltd.

Some of these interactions provide connections to larger scale morphological features such as folds and to the long edge and screw dislocation lines which were classified in polyethylene by Passaglia and Keith[8]. Folds are not considered explicitly in this paper because they intrinsically involve two chain stems and have a different relationship to the lattice than the defects listed above.

COMPUTATION OF MINIMUM ENERGY CONFORMATIONS

The minimum energy conformations and related parameters were calculated for crystallographic defects in polyethylene chains with 60 CH_2 units. These chains are long enough to essentially eliminate many, but not all, troublesome effects associated with the boundaries and yet are small enough to require reasonably short times on a contemporary supercomputer to compute the minimum energy conformations.

The model used for the crystallographic defects numbered above as (1), (2) and (3) had a central chain bearing the defect. The model is shown in *Figure 1*. The central chain was surrounded by 6 inner shell chains placed on lattice sites at the beginning of the calculation. The exact positions and conformations of the central chain and the six inner shell chains were adjusted to minimize the energy during the calculation.

These 6 inner shell chains were in turn surrounded by 12 additional chains on an outer shell, making a total of 19 chains in the model. The molecules in the outer shell were held in their all-*trans* conformation on the lattice sites throughout the calculation. Exploratory calculations showed that deflection of this rigid shell of molecules produced an effect on the energy of each defect that was small enough to be ignored.

The conformation of the central chain with the defect was adjusted to minimize its energy, subject to the constraint of the periodic potential created by the surrounding molecules that the chain must fit into the crystal lattice at large distances from the defect. Large distance means distances 2 to 3 times the extent of the clearly disordered region in the direction being considered.

Each all-*trans* chain contained exactly 60 carbon atoms and 122 hydrogen atoms since the chains were terminated with methyl groups. Defects which include extra atoms (interstitial-like), or fewer atoms (vacancy-like) change the number of atoms in the central chain. The ends of the central chain were constrained on lattice sites in exactly the same plane as the ends of the surrounding chains.

Every chain in the model used for the partial defects had an identical defect. This created a boundary which was placed at the middle of the 19 chain model shown in *Figure 1*. In these partial defect calculations the top half of the model and the bottom half were on crystallographic lattices that were displaced with respect to each other. When the conformation of one chain was changed during this calculation, all the other chains were changed in exactly the same way.

The computer program used to adjust all the conformations is based on a Newton–Raphson energy minimization algorithm and is the same program used in many earlier calculations[4]. It was run in a Cyber 205 computer. Running times ranged from about 5 min to as long as 20 min for the defects which produced the largest distortions of the model.

RESULTS

The energy required for each defect or partial defect is given in *Table 1* along with other results. *Figures 2–9* provide information about the distance from each carbon atom to a lattice site, and about the conformation of the defect bearing chains.

Appendix 1 contains tables which give the coordinates of each of the carbon atoms in each of the defect bearing chains. These tables may be used as the starting point for other calculations, or to examine the conformations in molecular graphics computer programs.

The excess energy associated with each defect was determined by subtracting the calculated energy of the all-

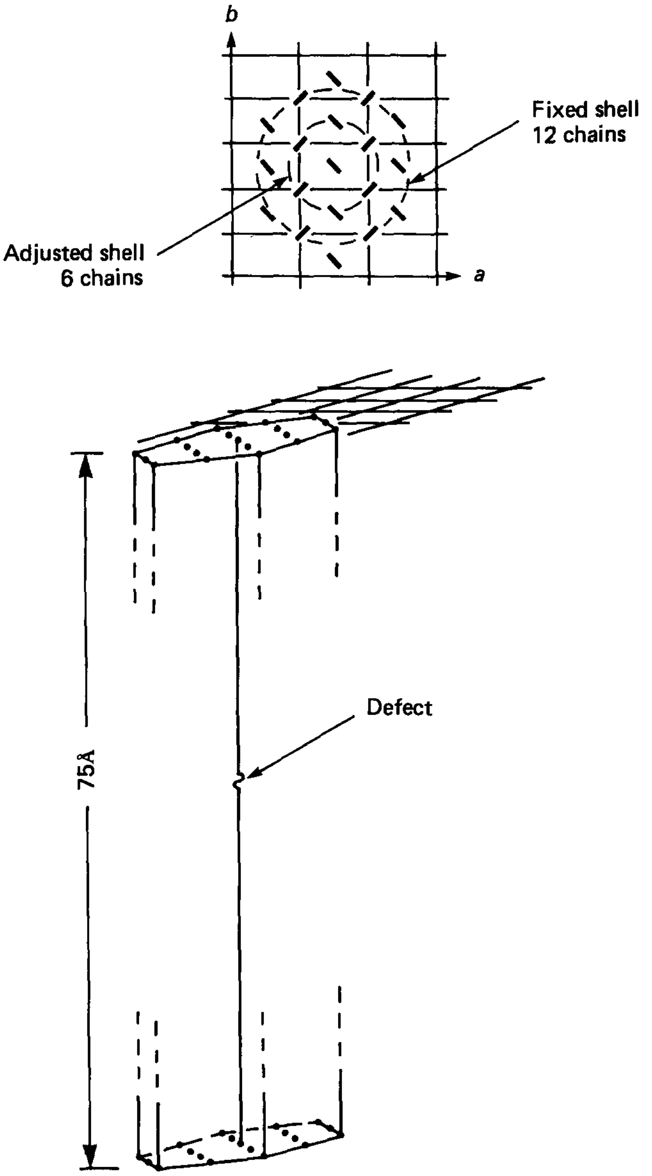

Figure 1 Diagram of the 19 chain model used for the calculations of minimum energy conformations of the defects. For the crystallographic defects, the central chain contained the defect, but for the partial defect boundaries all chains had the same conformation. The top part of the figure is viewed along the chain axis and shows the relationship of the chains to the orthorhombic unit cell. The lower view is from the side of the model

Table 1 Defects in a 60 C-atom long polyethylene crystal

Defect name	Length C-atoms	Energy (kcal mol^{-1})	E_c (kcal mol^{-1})
(1) Dispiration loop			
(a) interstitial-like	6	11.77	0.64
(b) vacancy-like	25	21.12	1.40
(2) Disclination loop	4	17.23	0.28
(3) Dislocation loop			
(a) interstitial-like	8	23.61	0.90
(b) vacancy-like	44	46.90	[a]
(4) Chain twist boundary (180°)			
(a) 180°	7.5	14.85	0.16
(b) 90°	4	7.81	0.25
(5) Partial dislocation boundary	8	7.6	1.8

[a] Unstable, not evaluated

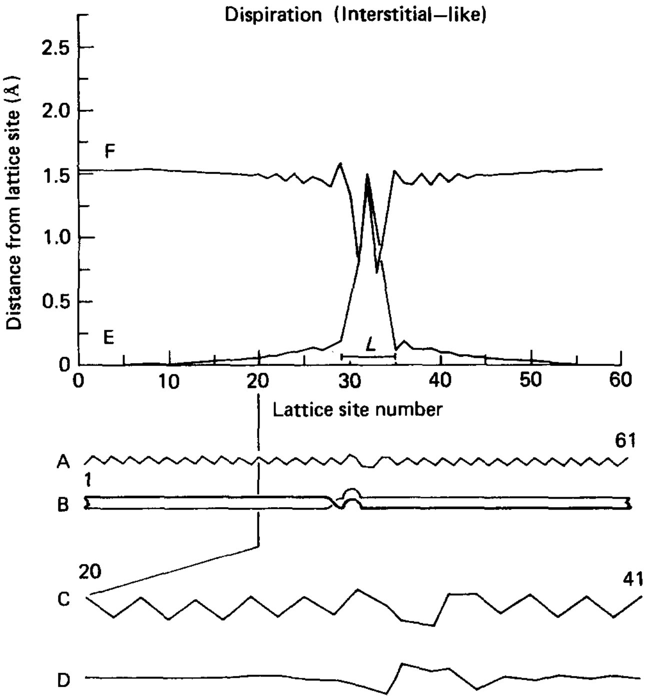

Figure 2 Diagrams of the interstitial-like dispiration in a polyethylene chain. (A) Positions of the carbon atoms in a segment containing 61 carbon atoms with a dispiration near its centre, so that the total length is exactly the same as the length of a zig-zag chain containing 60 carbon atoms. (B) A ribbon model of the chain. The dispiration can be represented as the combination of a partial disclination (180° twist) and a partial dislocation (extra CH_2). (C) View perpendicular to the zig-zag plane of a three times enlargement of the central part of the chain. (D) Similar enlargement viewed in the zig-zag plane. (E) A plot *versus* the lattice site number of the scalar distance between the position of a carbon atom in the defect bearing chain and a carbon atom crystal lattice site, with the first carbon atom of the defect bearing chain in register with the first lattice site. (F) Same as (E), but with the last carbon atom of the defect bearing chain aligned with the 60th lattice site

trans 19 chain model from the calculated energy of each of the defect bearing models. These values are summarized in *Table 1* in the column headed 'Energy'.

The energy listed in *Table 1* for a defect is that required to create the defect from a perfect crystal region. It provides a basis for estimating the concentration of that defect in thermal equilibrium with the crystal if a satisfactory estimate of the entropy is made. In a real sample the actual concentration of any particular kind of defect may be quite different because most of the defects are created from a non-equilibrium conformation of polyethylene. In a typical polyethylene sample there are folds, chain ends, or more complicated conformations which can participate in the defect creation process and lower the incremental energy required to form the defect. In addition, some defects are trapped in the crystal during crystallization. Others are created by mechanical deformation.

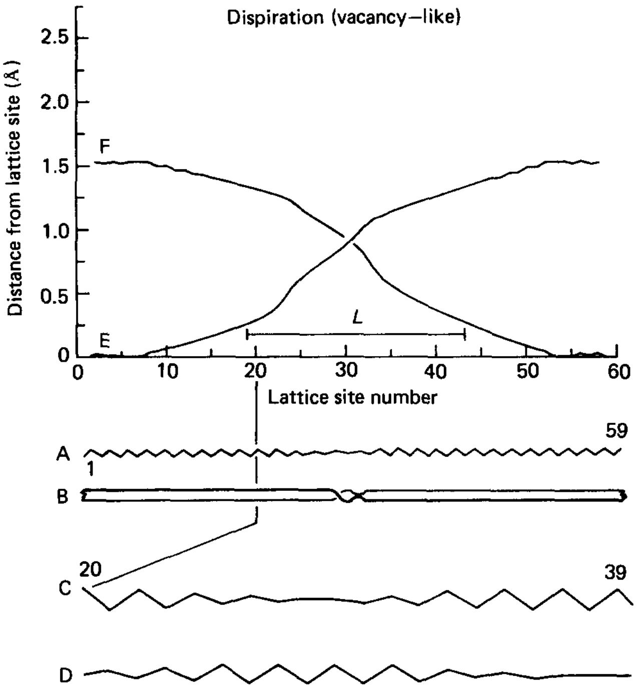

Figure 3 Diagrams of the vacancy-like dispiration. See caption of *Figure 2* for explanations. (B) shows that this crystallographic defect can be represented as the combination of a partial disclination (180° twist) and a vacancy-like partial dislocation

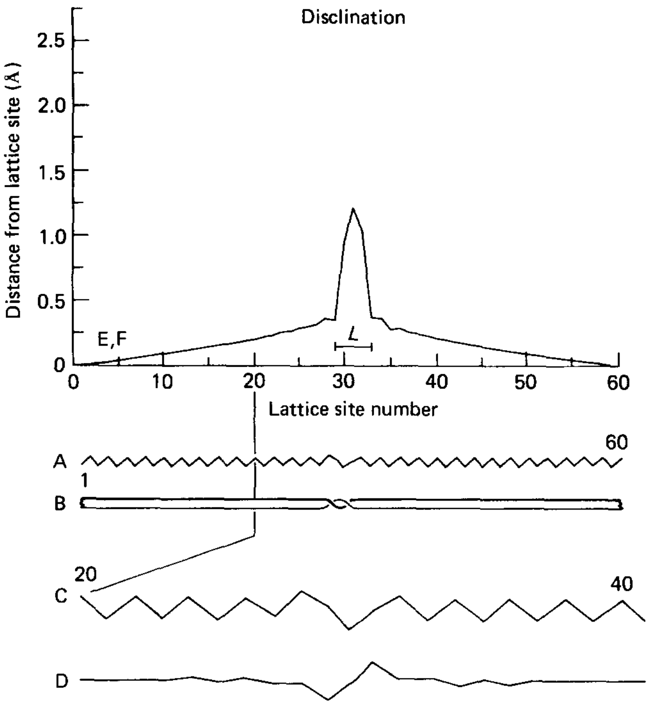

Figure 4 Diagrams of the disclination. See caption of *Figure 2* for explanations. (B) shows that this crystallographic defect can be represented as the combination of two partial disclinations (180° twist)

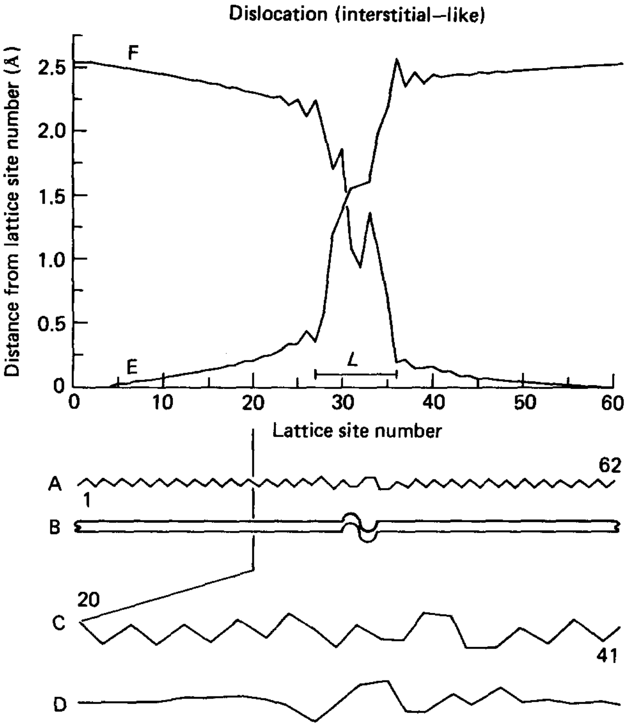

Figure 5 Diagrams of the interstitial-like dislocation. See caption of *Figure 2* for explanations. (B) shows that this crystallographic defect can be represented as the combination of two interstitial-like partial dislocations

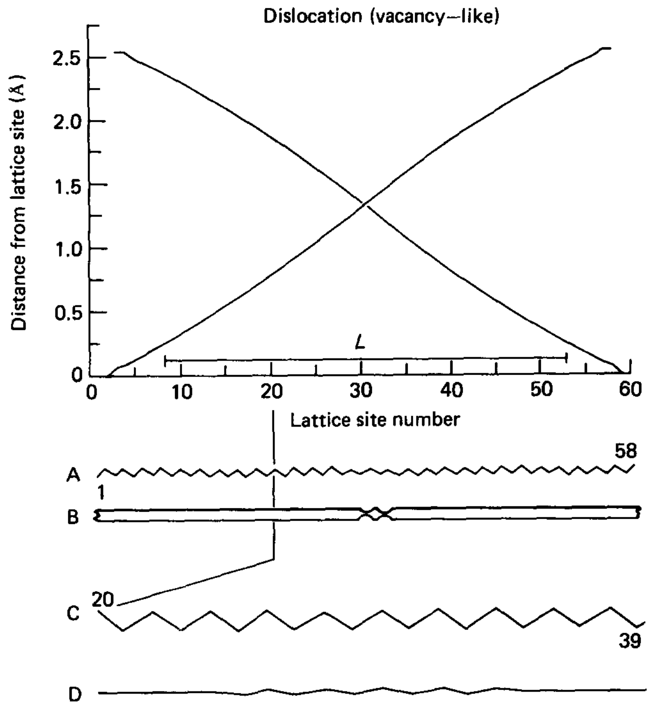

Figure 6 Diagrams of the vacancy-like dislocation. See caption of *Figure 2* for explanations. (B) shows that this crystallographic defect can be represented as the combination of two vacancy-like partial dislocations

The adequacy of the model for holding the carbon atoms on lattice sites near the ends of the chains in the model was examined. The condition that the end carbon atoms be on lattice sites was removed and the minimum energy conformation re-computed. If the crystal forces held the chain end exactly in this position, the energy would be the same as when the end atoms were constrained. The column headed 'E_c' in *Table 1* shows the energy differences actually calculated. In all cases, the energy of the constrained chain was higher.

Table 1 shows that E_c was small for the interstitial-like dispiration, the disclination and the chain twist boundaries, indicating that the model was long enough for an accurate calculation of the defect energy. For the vacancy-like dispiration, the interstitial dislocation, and the partial dislocation boundary, E_c is large and the

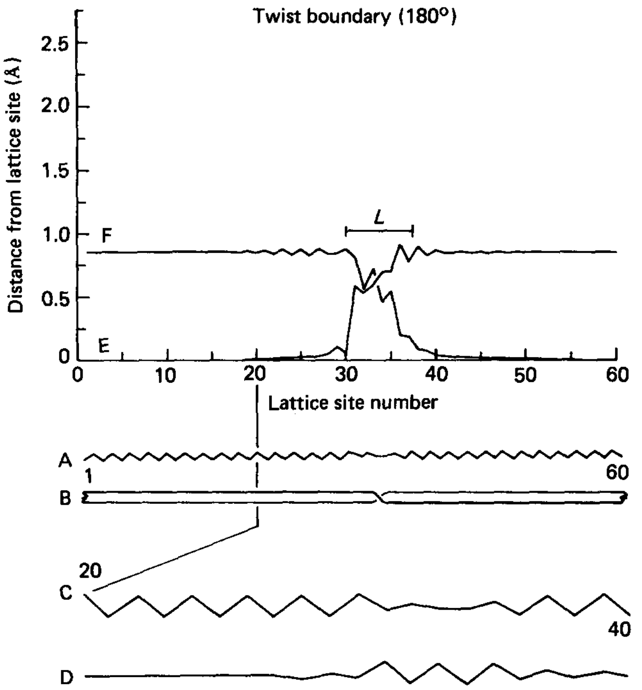

Figure 7 Diagrams of a typical chain that crosses a chain twist boundary with 180° twist. See caption of *Figure 2* for explanations. This chain contains a partial disclination with 180° twist

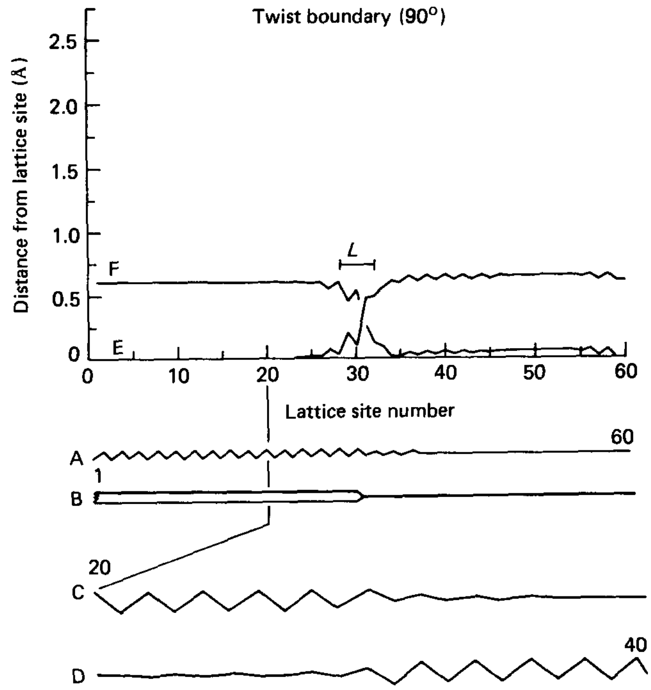

Figure 8 Diagrams of a typical chain that crosses a chain twist boundary with 90° twist. See caption of *Figure 2* for explanations. This chain contains a partial disclination with 90° twist

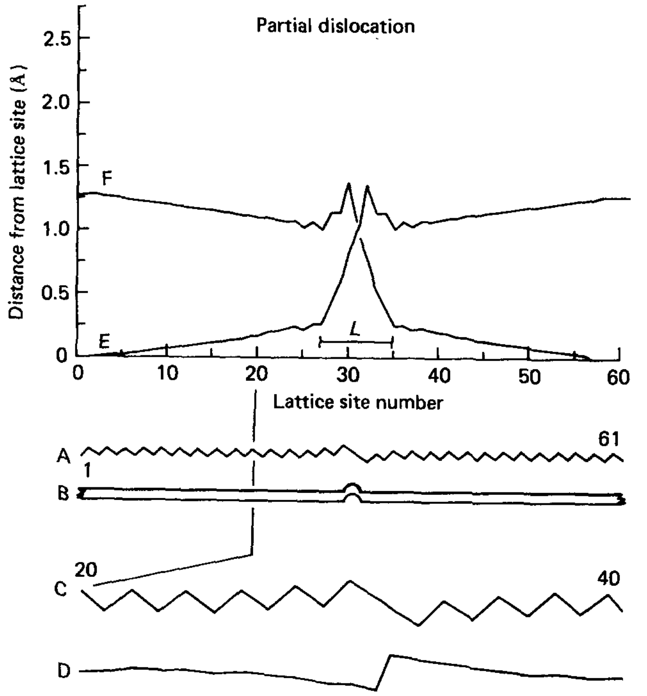

Figure 9 Diagrams of a typical chain that crosses a partial dislocation boundary. See caption of *Figure 2* for explanations. This chain contains an interstitial-like partial dislocation

calculated energies should be regarded as the best approximation available. The vacancy-like dislocation could not be maintained in this model without constraining the end atoms to lattice sites.

The length of each defect was evaluated from the graphs in *Figures 2* to *9*. These graphs show the magnitude of the distance from each carbon atom in the defect bearing chain to a lattice site. For each defect two curves are shown. For one curve a zig-zag chain representing the lattice sites and the defect bearing chain are aligned so that the *first* atoms in both chains are superimposed. For the second curve, the *last* carbon atoms in both chains are superimposed. This procedure produces a graph which displays the onset of the defect as it is approached from both directions along the chain. This method emphasizes the gradual increase of the actual atom positions away from the lattice sites as the defect is approached. It is a graphic alternative to the differentiation-like procedure that was used in earlier papers[4,9]. The value of the defect length given in *Table 1* is estimated from the graphs by considering both the positions at which the displacement curves turn sharply upward and the magnitude of the distances from the lattice sites as the defect is approached from either direction.

Figures 2 to *6* make it easy to judge how smoothly the defect-bearing chains fit back into the lattice of the 60 carbon atom long crystal used in the calculations. This is particularly striking for the vacancy-like dispiration and dislocation. The vacancy-like dispiration is longer than some defects but displays a gradual return to the lattice sites about 20 atom positions away from the centre of the defect. The vacancy-like dislocation had to be forced onto the lattice sites at the ends. This, along with the high value of E_c in *Table 1*, shows that the model is still too short to encompass the true length of the vacancy-like dislocation. A model at least 200 atom positions long would be required to show the full natural length of the vacancy-like dislocation.

DESCRIPTION OF EACH DEFECT

In this section each individual defect or partial defect is described. Each defect is characterized by its geometry, by the increase or decrease in the number of CH_2 groups in the defect region, and the amount of chain twist it involves. Part B of *Figures 2* to *9* shows a schematic diagram of each defect. Note that the crystallographic defects are represented as combinations of the partial defects. Parts C and D of *Figures 2* to *9* show projections of the bonds as viewed both in and perpendicular to the zig-zag plane. Some of the interesting changes in the position or orientation of the chain that result from the passage of each kind of defect are described. Leading references to previous papers are given.

Dispiration (interstitial-like)

A dispiration is a defect in the helical symmetry of a crystal. In polyethylene the interstitial-like dispiration contains one extra CH_2 group and the chain twists by 180° as it passes through the static defect.

Diffusion of the dispiration along the chain by Brownian motion both transports the chain and rotates it. The interstitial-like dispiration provides the simplest and lowest energy process to produce crystal thickening during annealing, although interactions with larger scale morphological features are necessary to produce the dramatic changes in stem length actually observed[1]. This dispiration can also provide the chain rotation needed to account for dielectric relaxation processes, certain satellite line broadening effects in the ^{13}C nuclear magnetic resonance spectrum of polyethylene[10] and some aspects of the alpha mechanical relaxation process[11]. The presence of this defect disrupts the longitudinal acoustic mode vibrations of the chain segment[12,13].

Dispiration (vacancy-like)

The vacancy-like dispiration contains one less CH_2 group than the perfect crystal and twists the molecule by 180°. The properties of the vacancy-like dispiration in a short chain segment were investigated by Mansfield and Boyd[2]. Its behaviour in a longer chain is found to be somewhat simpler. Its energy is significantly higher than that of the interstitial-like dispiration. Wahlstrand[3] attributed soliton-like motion to this defect and derived parameters from dielectric relaxation data. The vacancy-like dispiration does not disrupt the longitudinal acoustic mode vibrations of the chain segment since it contains no *gauche* dihedral angles.

Disclination

A disclination is a defect in the rotational symmetry of the crystal. In polyethylene the chain is twisted by 360° to produce a disclination. Diffusion of the disclination along the chain rotates the segment through which the disclination moves by 360°. It is useful for transport of the twist needed to resolve some kinds of morphological problems. Disclinations, in the lowest energy conformation found in this work, disrupt the longitudinal acoustic mode because they contain *gauche* dihedral angles which allow the axial strains associated with this mode to work against the soft rotational potential around bonds rather than against the stiff potential associated with the angle between adjacent bonds.

Dislocation (interstitial-like)

A dislocation is a defect in the translational symmetry of a crystal. The interstitial-like dislocation in polyethylene is an edge dislocation loop that encircles only one molecule. It has a Burger's vector of one repeat unit along the *c* axis and therefore contains two extra CH_2 groups. This dislocation requires a relatively large distorted region both along the chain and in the surrounding inner shell chains to accommodate the two extra groups. Passage of this dislocation transports the chain along its axis in steps equal to the crystallographic repeat distance without rotating the chain. The absence of rotation may be important in some mechanisms, for example when a side group is forced inside the crystal during mechanical deformation. The dislocation disrupts the longitudinal acoustic mode of the segment of the molecule in which it resides.

Dislocation (vacancy-like)

This defect is also an edge dislocation loop but the 'extra half-plane' referred to in elementary treatments of edge dislocations is now outside the loop rather than inside it as is the case for the interstitial-like dislocation. The central chain retains its planar zig-zag conformation, but the angle between the bonds in the vicinity of the defect is significantly increased. Since the energy required to increase this angle is large the defect spreads over a greater distance along the chain. The longitudinal acoustic mode is not disrupted by the vacancy-like dislocation. The energy of this defect is so high that very few would be expected to be created by thermal excitation, but it may be important in translating the chain in a stress field that stretches the chain. The vacancy-like dislocation provides a way to relieve the stress by allowing the chain to move along its axis, and thus may delay or eliminate chain breaking. The vacancy-like dispiration also provides a similar transport mechanism at lower energy, but dispirations require chain rotation which may introduce complications, for example in the vicinity of a side branch.

Chain twist boundary (180°)

In polyethylene, a localized 180° twist in a chain is a partial disclination. Partial defects provide a useful way of thinking about the relationship and interaction of defects, but partial defects do not fit into the lattice. It is possible for partial defects to form a boundary between two crystal grains[4] if every chain crossing the boundary contains a partial defect at the boundary. This possibility in polyethylene has a reasonably low energy and provides a mechanism for localizing adventitious twist captured in the chain during crystallization. This was suggested[4] as the first step in the creation of the long period in polymer fibres that is observed in X-ray diffraction data. An infrared band occurring near 680 wavenumbers was assigned to the presences of twist boundaries[14]. Motion of a chain twist boundary rotates the segment of each chain crossing the boundary by 180°. This boundary motion was proposed[15] as a possible mechanism for reversing the polarity of the piezoelectric polymer, poly(vinylidene fluoride), which has a crystal structure similar to that of polyethylene.

Chain twist boundary (90°)

The 90° chain twist boundary consists of a 90° partial disclination in each chain. This is a relatively low energy boundary. It produces a 90° rotation of the *a* and *b* unit cell directions. It can accommodate adventitious twist present in a molecule and contribute to the formation of the long period in a fibre.

Partial dislocation boundary

A partial dislocation boundary has an extra CH_2 group in every chain at the point the chain passes through the boundary. A partial dislocation boundary was created by constraining the ends of a chain containing 61 carbon atoms at the position appropriate for the ends of a 60 atom chain in the all-*trans* conformation. This boundary proved to be stable even when the end constraints were removed, but the barrier to its disappearance (with a simultaneous lengthening of the chain) was estimated to be only 3 kcal mol^{-1}. The chains that passed through the partial dislocation boundary were 0.46 Å longer when the end constraints were removed, but some of the dihedral angles remained in the *gauche* wells.

REMARKS

There is a 'chemistry' of interactions between defects. For example, dispirations can be created and annihilated at folds or chain ends. An accurate estimate of the number of any particular kind of defect must take this 'chemistry' into account, but the information needed to do so is sparse and only becoming available now. Reneker and Mazur[4], for example, examined the interaction between a chain twist boundary and an interstitial-like dispiration.

A partial disclination can be converted to a partial dislocation if a dispiration with a cancelling twist arrives at the chain twist boundary composed of partial disclinations. The twist at the boundary is then cancelled by that of the dispiration but the extra CH_2 carried by the dispiration is left behind in the boundary as a partial dislocation.

One important property of the vacancy-like defects which deserves emphasis is their ability to transport free volume in the crystal. This is likely to be very important in the establishment of the 'long period' morphology of fibres[4] since X-ray diffraction shows that there are periodically distributed regions of lower density, implying that free volume migrates through the crystal during thermal treatment which changes the long period.

In a small fibre in which the boundary crosses the entire fibre, partial defect boundaries can be thought of as a kind of grain boundary, which is the viewpoint assumed here. Changes in the number of partial dislocation boundaries in a small fibre could produce significant changes in the length of the fibre.

The partial disclination boundaries and the partial dislocation boundary are each part of a structure called a stacking fault. If the partial defect boundaries described above are embedded in a large crystal an additional energy associated with the edges of the stacking fault must be considered. This step is not included in this paper.

It is not the purpose of this paper to summarize the history of the development of this family of defects in polyethylene in detail, but some early work which influenced the development of the above ideas is mentioned. Pechhold[16] described defects to explain mechanical relaxation effects but these defects were not in minimum energy conformations and the chain did not always return to lattice sites at large distances from the defect. Minimum energy conformations were calculated for a later defect model made by his associates[17] but in the terms used in this paper, the conformations modelled were combinations of partial defects which do not make crystallographic defects that fit into the lattice. Some of the combinations are very unstable because the partial defects can combine with each other, reducing the energy and leaving a planar zig-zag.

Weber and Helfand[18] have modelled the motions of the crankshaft conformation. The molecular dynamics approach they used, which is very incisive in detail, shows promise of being extended with larger computers and improved algorithms to times long enough that the kind of diffusive motion that is natural for the above crystallographic defects can be observed[19].

CONCLUSIONS

The known family of crystallographic defects which involve only a single chain was described. These nanometre scale molecular mechanisms are able to perform many functions that involve rotation or translation of a single chain. They are part of a larger family of topologically similar defects which involve two or more chains. The defect loops can be extended to encircle more chains. The dislocations described here are the small limit of the dislocation lines considered by Keith and Passaglia[8]. Modelling of the interaction of the defects with each other and with morphological features such as folds or 'impurity' structures such as branches offers a way to an improved understanding of the larger scale mechanical and physical properties of crystalline polyethylene.

REFERENCES

1 Reneker, D. H. *J. Polym. Sci.* 1962, **S59**, 539
2 Mansfield, M. and Boyd, R. H. *J. Polym. Sci., Polym. Phys. Edn.* 1978, **16**, 1227
3 Wahlstrand, K. J. *J. Chem. Phys.* 1985, **82**, 5247
4 Reneker, D. H. and Mazur, J. *Polymer* 1983, **24**, 1387
5 Kausch, H. H., private communication
6 Reneker, D. H. and Mazur, J. *J. Phys. (Paris)* 1985, **46**, C10-499
7 Predecki, P. and Statton, W. O. *J. Appl. Phys.* 1966, **37**, 4053
8 Keith, H. D. and Passaglia, E. *J. Res. Natl. Bur. Stand.* 1968, **68A**, 513
9 Reneker, D. H., Fanconi, B. M. and Mazur, J. *J. Appl. Phys.* 1977, **48**, 4032
10 Vanderhart, D. L. *J. Magn. Res.* 1976, **24**, 467
11 Reneker, D. H. and Mazur, J. *Polymer* 1982, **23**, 401
12 Reneker, D. H. and Mazur, J. *Polymer* 1984, **25**, 1549
13 Mazur, J., Reneker, D. H. and Fanconi, B. M. *Polymer* 1987, **28** (*Commun.*), 78
14 Reneker, D. H., Mazur, J. and Fanconi, B. M. *Polymer* 1985, **26** (*Commun.*), 332
15 Reneker, D. H. and Mazur, J. *Polymer* 1985, **26**, 821
16 Pechhold, W., Blasenbrey, S. and Woerner, S. *Kolloid Z.* 1963, **189**, 14
17 Scherr, H., Hagele, P. C. and Grossman, H. P. *Colloid Polym. Sci.* 1974, **252**, 871
18 Weber, T. A. and Helfand, E. *Bull. Am. Phys. Soc.* 1983, **28**, 473 (Abstract HR7)
19 Noid, D. W. and Pfeffer, G. A. *Bull. Am. Phys. Soc.* 1987, **32**, 667 (Abstract JU28)

APPENDIX 1

Cartesian coordinates of carbon atom positions

(1) Dispiration (Interstitial-like)

Carbon atom numbers	*X*	*Y*	*Z*
1	−0.428	0.000	0.000
2	0.428	0.000	1.268
3	−0.428	0.000	2.537
4	0.428	0.000	3.806
5	−0.428	0.000	5.074
6	0.428	0.000	6.341
7	−0.438	−0.004	7.603
8	0.425	0.002	8.867
9	−0.439	−0.004	10.131
10	0.425	0.004	11.394
11	−0.438	−0.005	12.658
12	0.426	0.006	13.921
13	−0.437	−0.003	15.185
14	0.428	0.006	16.447
15	−0.434	−0.002	17.712
16	0.434	0.005	18.972
17	−0.423	−0.004	20.239
18	0.451	−0.002	21.495
19	−0.400	−0.012	22.767
20	0.479	−0.022	24.019
21	−0.370	−0.025	25.291
22	0.506	−0.051	26.546
23	−0.355	−0.012	27.807
24	0.491	−0.054	29.083
25	−0.405	0.132	30.306
26	0.356	0.028	31.630
27	−0.547	0.503	32.772
28	−0.510	−0.381	34.012
29	0.823	−0.320	34.764
30	0.609	−0.582	36.260
31	−0.032	0.634	36.935
32	−0.699	0.300	38.265
33	0.295	0.087	39.409
34	−0.471	−0.042	40.727
35	0.452	−0.066	41.945
36	−0.382	−0.080	43.229
37	0.492	−0.051	44.482
38	−0.376	−0.041	45.743
39	0.478	−0.014	47.010
40	−0.398	−0.011	48.264
41	0.454	0.004	49.534
42	−0.419	−0.002	50.790
43	0.437	0.007	52.057
44	−0.431	−0.001	53.316
45	0.430	0.006	54.581
46	−0.436	−0.003	55.843
47	0.428	0.004	57.106
48	−0.435	−0.003	58.369
49	0.429	0.004	59.632
50	−0.434	−0.003	60.896
51	0.431	0.004	62.158
52	−0.431	−0.002	63.422
53	0.435	0.003	64.684
54	−0.428	0.000	65.949
55	0.428	0.000	67.225
56	−0.428	0.000	68.494
57	0.428	0.000	69.762
58	−0.428	0.000	71.030
59	0.428	0.000	72.298
60	−0.428	0.000	73.567
61	0.428	0.000	74.835

(2) Dispiration (vacancy-like)

Carbon atom number	*X*	*Y*	*Z*
1	−0.428	0.000	0.000
2	0.428	0.000	1.269
3	−0.404	−0.004	2.537
4	0.441	0.002	3.806
5	−0.402	−0.005	5.074
6	0.436	0.004	6.342
7	−0.428	0.000	7.611
8	0.428	0.000	8.879
9	−0.404	−0.004	10.183
10	0.441	0.002	11.474
11	−0.402	−0.005	12.768
12	0.436	0.004	14.065
13	−0.409	−0.007	15.357
14	0.429	0.006	16.655
15	−0.415	−0.008	17.948
16	0.423	0.009	19.246
17	−0.418	−0.011	20.542
18	0.421	0.013	21.840
19	−0.419	−0.016	23.138
20	0.419	0.020	24.437
21	−0.418	−0.025	25.736
22	0.417	0.033	27.037
23	−0.416	−0.047	28.338
24	0.411	0.063	29.641
25	−0.409	−0.097	30.943
26	0.390	0.140	32.248
27	−0.370	−0.210	33.551
28	0.274	0.323	34.853
29	−0.146	−0.401	36.155
30	0.059	0.411	37.457
31	0.002	−0.420	38.761
32	−0.052	0.413	40.064
33	0.092	−0.408	41.367
34	−0.135	0.395	42.670
35	0.188	−0.375	43.972
36	−0.261	0.331	45.271
37	0.355	−0.235	46.569
38	−0.400	0.142	47.862
39	0.410	−0.086	49.157
40	−0.421	0.050	50.450
41	0.419	−0.026	51.743
42	−0.423	0.014	53.035
43	0.422	−0.005	54.326
44	−0.422	0.001	55.617
45	0.425	0.002	56.907
46	−0.419	−0.003	58.198
47	0.429	0.003	59.485
48	−0.413	−0.004	60.776
49	0.436	0.003	62.063
50	−0.407	−0.004	63.353
51	0.440	0.002	64.641
52	−0.408	−0.003	65.927
53	0.428	0.000	67.224
54	−0.428	0.000	68.492
55	0.436	0.003	69.760
56	−0.407	−0.004	71.029
57	0.440	0.002	72.297
58	−0.408	−0.003	73.566
59	0.428	0.000	74.834

(3) Disclination

Carbon atom number	*X*	*Y*	*Z*
1	−0.428	0.000	0.000
2	0.428	0.000	1.268
3	−0.422	−0.003	2.550
4	0.434	0.002	3.826
5	−0.420	−0.004	5.104
6	0.432	0.003	6.382
7	−0.423	−0.004	7.659
8	0.430	0.004	8.938
9	−0.424	−0.004	10.216
10	0.428	0.004	11.494
11	−0.425	−0.005	12.773
12	0.428	0.005	14.052
13	−0.425	−0.005	15.330
14	0.427	0.006	16.610
15	−0.427	−0.005	17.889
16	0.424	0.007	19.170
17	−0.431	−0.004	20.449
18	0.417	0.007	21.733
19	−0.440	−0.006	23.010
20	0.404	0.003	24.296
21	−0.453	−0.012	25.574
22	0.391	−0.014	26.861
23	−0.461	−0.029	28.144
24	0.395	−0.049	29.422
25	−0.431	−0.036	30.723
26	0.461	−0.071	31.975
27	−0.295	0.078	33.311
28	0.673	0.081	34.512
29	0.172	0.811	35.767
30	−0.770	0.058	36.706
31	−0.065	−0.796	37.762
32	0.520	−0.088	38.995
33	−0.388	−0.100	40.242
34	0.408	0.092	41.549
35	−0.452	0.023	42.824
36	0.390	0.074	44.114
37	−0.454	0.018	45.400
38	0.400	0.037	46.681
39	−0.442	0.001	47.969
40	0.413	0.017	49.249
41	−0.432	−0.006	50.535
42	0.422	0.009	51.815
43	−0.427	−0.007	53.098
44	0.426	0.006	54.378
45	−0.425	−0.007	55.660
46	0.427	0.005	56.940
47	−0.425	−0.006	58.220
48	0.427	0.005	59.500
49	−0.426	−0.005	60.779
50	0.426	0.005	62.058
51	−0.427	−0.004	63.337
52	0.425	0.004	64.616
53	−0.430	−0.004	65.894
54	0.422	0.004	67.173
55	−0.432	−0.003	68.450
56	0.420	0.004	69.729
57	−0.434	−0.002	71.007
58	0.421	0.003	72.284
59	−0.428	0.000	73.565
60	0.428	0.000	74.834

(4) Dislocation (interstitial-like)

Carbon atom number	X	Y	Z
1	−0.428	0.000	0.000
2	0.428	0.000	1.268
3	−0.436	−0.002	2.531
4	0.427	0.002	3.796
5	−0.436	−0.002	5.060
6	0.429	0.001	6.323
7	−0.432	−0.002	7.588
8	0.433	0.001	8.851
9	−0.429	−0.001	10.116
10	0.436	0.001	11.379
11	−0.426	−0.002	12.643
12	0.437	0.000	13.907
13	−0.427	−0.003	15.169
14	0.433	−0.001	16.435
15	−0.437	−0.002	17.694
16	0.416	−0.001	18.964
17	−0.462	0.005	20.217
18	0.383	0.009	21.492
19	−0.501	0.029	22.741
20	0.344	0.029	24.014
21	−0.531	0.071	25.271
22	0.338	0.023	26.526
23	−0.488	0.091	27.815
24	0.434	−0.133	29.011
25	−0.256	0.012	30.370
26	0.656	−0.595	31.439
27	0.578	0.054	32.811
28	−0.707	−0.290	33.565
29	−0.834	0.526	34.853
30	0.365	0.415	35.797
31	0.304	−0.890	36.593
32	−0.349	−0.664	37.955
33	0.635	0.028	38.904
34	−0.134	0.898	39.882
35	−0.765	0.153	41.045
36	0.260	−0.100	42.152
37	−0.483	−0.251	43.474
38	0.465	−0.195	44.667
39	−0.366	−0.166	45.947
40	0.518	−0.077	47.184
41	−0.359	−0.043	48.433
42	0.497	0.002	49.693
43	−0.392	0.006	50.935
44	0.462	0.020	52.199
45	−0.422	0.009	53.443
46	0.438	0.012	54.704
47	−0.438	0.002	55.955
48	0.429	0.005	57.212
49	−0.441	−0.002	58.467
50	0.428	0.001	59.722
51	−0.438	−0.003	60.979
52	0.433	0.001	62.234
53	−0.432	−0.002	63.492
54	0.439	0.002	64.747
55	−0.426	−0.001	66.006
56	0.445	0.005	67.261
57	−0.421	0.000	68.519
58	0.445	0.006	69.778
59	−0.428	0.000	71.030
60	0.428	0.000	72.299
61	−0.428	0.000	73.568
62	0.428	0.000	74.836

(5) Dislocation (vacancy-like)

Carbon atom number	X	Y	Z
1	−0.428	0.000	0.000
2	0.428	0.000	1.268
3	−0.392	−0.004	2.587
4	0.445	0.003	3.889
5	−0.391	−0.007	5.194
6	0.438	0.005	6.502
7	−0.401	−0.009	7.805
8	0.427	0.008	9.115
9	−0.409	−0.012	10.420
10	0.420	0.012	11.730
11	−0.413	−0.015	13.037
12	0.417	0.016	14.348
13	−0.414	−0.020	15.658
14	0.415	0.021	16.970
15	−0.413	−0.025	18.282
16	0.413	0.026	19.596
17	−0.412	−0.030	20.910
18	0.412	0.032	22.226
19	−0.411	−0.035	23.543
20	0.411	0.038	24.860
21	−0.410	−0.040	26.179
22	0.410	0.043	27.498
23	−0.409	−0.044	28.818
24	0.408	0.047	30.140
25	−0.408	−0.048	31.461
26	0.407	0.050	32.784
27	−0.407	−0.050	34.106
28	0.407	0.052	35.429
29	−0.407	−0.051	36.753
30	0.407	0.052	38.076
31	−0.407	−0.051	39.399
32	0.407	0.051	40.722
33	−0.408	−0.049	42.045
34	0.408	0.048	43.368
35	−0.408	−0.046	44.689
36	0.409	0.045	46.010
37	−0.409	−0.043	47.331
38	0.410	0.041	48.650
39	−0.410	−0.038	49.970
40	0.411	0.036	51.287
41	−0.411	−0.033	52.604
42	0.413	0.027	53.920
43	−0.413	−0.027	55.235
44	0.414	0.024	56.549
45	−0.414	−0.022	57.861
46	0.414	0.019	59.173
47	−0.416	−0.017	60.484
48	0.413	0.015	61.795
49	−0.420	−0.012	63.103
50	0.409	0.011	64.413
51	−0.427	−0.009	65.718
52	0.401	0.009	67.029
53	−0.437	−0.005	68.332
54	0.391	0.007	69.640
55	−0.445	−0.003	70.946
56	0.393	0.005	72.248
57	−0.428	0.000	73.567
58	0.428	0.000	74.835

(6) Chain twist boundary (180°)

Carbon atom number	*X*	*Y*	*Z*
1	−0.428	0.000	0.000
2	0.428	0.000	1.268
3	−0.431	−0.003	2.539
4	0.429	0.002	3.808
5	−0.430	−0.003	5.078
6	0.430	0.003	6.347
7	−0.430	−0.003	7.617
8	0.430	0.003	8.886
9	−0.429	−0.003	10.156
10	0.431	0.004	11.426
11	−0.427	−0.003	12.696
12	0.433	0.004	13.965
13	−0.425	−0.004	15.235
14	0.435	0.003	16.504
15	−0.423	−0.005	17.775
16	0.436	0.004	19.044
17	−0.424	−0.007	20.314
18	0.434	0.007	21.585
19	−0.429	−0.011	22.852
20	0.424	0.020	24.126
21	−0.443	−0.028	25.389
22	0.398	0.056	26.668
23	−0.469	−0.077	27.925
24	0.336	0.159	29.207
25	−0.472	−0.193	30.462
26	0.112	0.444	31.726
27	−0.160	−0.378	32.992
28	−0.109	0.495	34.250
29	0.018	−0.332	35.535
30	−0.182	0.538	36.782
31	0.454	−0.048	38.046
32	−0.415	0.102	39.301
33	0.413	−0.049	40.583
34	−0.453	−0.002	41.846
35	0.403	−0.024	43.118
36	−0.455	−0.007	44.388
37	0.407	−0.001	45.656
38	−0.449	0.002	46.928
39	0.415	0.009	48.194
40	−0.441	0.004	49.466
41	0.422	0.009	50.733
42	−0.435	0.002	52.004
43	0.427	0.006	53.271
44	−0.431	−0.002	54.541
45	0.430	0.003	55.809
46	−0.430	−0.004	57.078
47	0.431	0.001	58.347
48	−0.429	−0.004	59.615
49	0.431	0.000	60.884
50	−0.429	−0.002	62.152
51	0.432	−0.004	63.420
52	−0.429	0.004	64.689
53	0.432	0.000	65.957
54	−0.429	0.001	67.225
55	0.430	0.002	68.493
56	−0.431	−0.002	69.761
57	0.429	0.002	71.029
58	−0.432	−0.002	72.297
59	0.428	0.000	73.565
60	−0.428	0.000	74.834

(7) Chain twist boundary (90°)

Carbon atom number	*X*	*Y*	*Z*
1	0.000	−0.428	0.000
2	0.000	0.428	1.268
3	0.074	−0.429	2.537
4	−0.017	0.426	3.805
5	0.073	−0.428	5.074
6	−0.045	0.425	6.342
7	0.065	−0.427	7.611
8	−0.060	0.425	8.879
9	0.061	−0.426	10.148
10	−0.062	0.425	11.417
11	0.059	−0.427	12.685
12	−0.057	0.423	13.954
13	0.056	−0.432	15.221
14	−0.050	0.419	16.492
15	0.055	−0.438	17.759
16	−0.041	0.414	19.029
17	0.049	−0.443	20.297
18	−0.031	0.414	21.566
19	0.053	−0.442	22.835
20	−0.027	0.413	24.104
21	0.055	−0.443	25.373
22	−0.024	0.412	26.643
23	0.052	−0.444	27.912
24	−0.015	0.413	29.180
25	0.041	−0.442	30.452
26	0.011	0.423	31.717
27	0.007	−0.426	32.993
28	0.084	0.447	34.251
29	−0.099	−0.370	35.534
30	0.251	0.444	36.784
31	−0.429	−0.096	38.046
32	0.384	0.192	39.313
33	−0.444	−0.027	40.585
34	0.415	0.070	41.850
35	−0.436	−0.013	43.123
36	0.427	0.021	44.390
37	−0.430	−0.011	45.660
38	0.430	0.005	46.929
39	−0.429	−0.009	48.198
40	0.431	0.001	49.467
41	−0.429	−0.007	50.736
42	0.430	0.003	52.004
43	−0.429	−0.005	53.273
44	0.432	0.007	54.541
45	−0.427	−0.004	55.810
46	0.433	0.005	57.078
47	−0.427	−0.004	58.346
48	0.432	0.004	59.615
49	−0.429	−0.004	60.883
50	0.431	0.003	62.151
51	−0.430	−0.003	63.419
52	0.430	0.003	64.688
53	−0.430	−0.003	65.956
54	0.430	0.003	67.224
55	−0.430	−0.003	68.492
56	0.431	0.003	69.760
57	−0.429	−0.002	71.029
58	0.432	0.003	72.297
59	−0.428	0.000	73.565
60	0.428	0.000	74.834

(8) Partial dislocation (Interstitial-like)

Carbon atom number	*X*	*Y*	*Z*
1	0.428	0.000	0.000
2	−0.428	0.000	1.268
3	0.430	0.002	2.536
4	−0.427	0.000	3.804
5	0.447	0.001	5.051
6	−0.420	−0.006	6.311
7	0.445	0.000	7.570
7	−0.423	−0.006	8.828
9	0.442	0.001	10.088
10	−0.426	−0.006	11.346
11	0.440	0.000	12.606
12	−0.427	−0.007	13.864
13	0.438	−0.001	15.124
14	−0.431	−0.008	16.381
15	0.433	−0.001	17.642
16	−0.440	−0.005	18.896
17	0.419	0.005	20.160
18	−0.460	0.006	21.410
19	0.394	0.025	22.677
20	−0.488	0.032	23.926
21	0.367	0.056	25.191
22	−0.506	0.060	26.446
23	0.366	0.075	27.698
24	−0.479	0.043	28.972
25	0.433	0.020	30.197
26	−0.360	−0.093	31.498
27	0.605	−0.176	32.680
28	−0.129	−0.370	34.005
29	0.887	−0.505	35.141
30	0.229	−0.660	36.510
31	−0.273	0.670	37.068
32	−0.925	0.517	38.439
33	0.096	0.387	39.571
34	−0.628	0.190	40.901
35	0.345	0.106	42.076
36	−0.440	−0.013	43.381
37	0.477	−0.039	44.602
38	−0.364	−0.075	45.878
39	0.510	−0.062	47.129
40	−0.363	−0.058	48.384
41	0.491	−0.034	49.649
42	−0.391	−0.026	50.898
43	0.462	−0.007	52.165
44	−0.418	−0.005	53.415
45	0.440	0.006	54.679
46	−0.433	0.002	55.933
47	0.430	0.008	57.194
48	−0.439	0.001	58.451
49	0.427	0.007	59.710
50	−0.441	0.000	60.968
51	0.425	0.006	62.228
52	−0.443	0.000	63.486
53	0.423	0.007	64.745
54	−0.446	0.000	66.003
55	0.419	0.006	67.263
56	−0.448	−0.002	68.522
57	0.421	0.001	69.779
58	−0.433	−0.003	71.043
59	0.428	−0.004	72.292
60	−0.428	0.000	73.565
61	0.428	0.000	74.836